From Scalar-Valued Images to Hypercomplex Representations and Derived Total Orderings for Morphological Operators

Jesús Angulo

CMM-Centre de Morphologie Mathématique, Mathématiques et Systèmes, MINES Paristech; 35, rue Saint Honoré, 77305 Fontainebleau Cedex, France
{jesus.angulo}@ensmp.fr

Abstract. In classical mathematical morphology for scalar images, the natural ordering of grey levels is used to define the erosion/dilation and the derived operators. Various operators can be sequentially applied to the resulting images always using the same ordering. In this paper we propose to consider the result of a prior transformation to define the imaginary part of a complex image, where the real part is the initial image. Then, total orderings between complex numbers allow defining subsequent morphological operations between complex pixels. In this case, the operators take into account simultaneously the information of the initial image and the processed image. In addition, the approach can be generalised to the hypercomplex representation (i.e., real quaternion) by associating to each image three different operations, for instance a directional filter. Total orderings initially introduced for colour quaternions are used to define the derived morphological transformations. Effects of these new operators are illustrated with different examples of filtering.

1 Introduction

Let $f(\mathbf{x}) = t$ be a scalar image, $f : E \rightarrow \mathcal{T}$. In general $t \in \mathcal{T} \subset \mathbb{Z}$ or $\mathbb{R}$, but for the sake of simplicity of our study, $\mathcal{T} = \{0, 1, \cdots, t_{\max}\}$ (e.g., $t_{\max} = 255$ for 8 bits images) is considered as an ordered set of grey-levels; and typically, for digital 2D images $\mathbf{x} = (x, y) \in E$ where $E \subset \mathbb{Z}^2$ is the support of the image. For 3D images $\mathbf{x} = (x, y, z) \in E \subset \mathbb{Z}^3$. According to the natural scalar partial ordering $\leq$, $\mathcal{T}$ is a complete lattice, and then $\mathcal{F}(E, \mathcal{T})$ is a complete lattice too. Morphological operators are naturally defined in the framework of functions $\mathcal{F}(E, \mathcal{T})$ [15,16,9]. Various operators can be sequentially applied to the resulting images always using the same ordering $\leq$.

The aim of this paper is to construct (hyper)-complex image representations which will be endowed with total orderings and consequently, which will lead to complete lattices. More precisely, it is proposed to use the result of a prior morphological transformation to define the imaginary part of a complex image, where the real part is the initial scalar image. Then, total orderings between complex numbers allow defining subsequent morphological operations between

M.H.F. Wilkinson and J.B.T.M. Roerdink (Eds.): ISMM 2009, LNCS 5720, pp. 238–249, 2009.

complex pixels. In this case, the operators take into account simultaneously the scalar intensities of both the initial and the transformed images. The complex scalar value brings information about the invariance of intensities with respect to a particular size and shape structure (i.e., using openings, closings or alternate sequential filters) as well as information about the local contrast of intensities (i.e., by means of top-hat transformations). In addition, the approach is then generalised to the hypercomplex representation (i.e., real quaternion) by associating to each image three different operations, for instance a series directional filters.

The motivation of these methodological developments is to obtain "regularized" morphological operators whose result depends not only on the sup/inf of the grey values, locally computed in the structuring element, but also on differential information or more regional information. The problem has been previously addressed using an inf-semilattice framework [10], working on fuzzy logic morphology [4] or introducing microviscous effects by second-order operators [13].

Geometric algebraic representations have been previously used for image modelling and processing. Classically, in one-dimensional (1D) signal processing, the analytic signal is a powerful complex-model which provides access to local amplitude and phase. The complex signal is built from a real signal by adding its Hilbert transform -which is a phase-shifted version of the signal- as an imaginary part to the signal. The approach was extended to 2D signals and images in [3] by means of the quaternionic Fourier transform. In parallel, another theory introduced in [7] to extend the analytic model in 2D is based on the application of the Riesz transform as generalised Hilbert transform, leading to the notion of monogenic signal which delivers an orthogonal decomposition into amplitude, phase and orientation. Later, the monogenic signal was studied in the framework of scale-spaces [8]. More recently, in [19], the 2D scalar-valued images are embedded into the geometric algebra of the Euclidean 4D space and then the structure are decomposed using monogenic curvature tensor. The quaternion-based representations have been also used to deal with colour image processing, such as colour Fourier transform, colour convolution and linear filters, have been studied mainly by [5,14,6], and to build colour PCA by [18]. We have recently explored also the interest of colour quaternions for extending mathematical morphology to colour images [2].

2 Complex Representation, Total Orderings and Complex Operators

Let $\psi : \mathcal{T} \rightarrow \mathcal{T}$ be a morphological operator for scalar images. We need to recall a few notions which characterise the properties of morphological operators. ψ is increasing if $\forall f, g \in \mathcal{F}(E, \mathcal{T})$, $f \leq g \Rightarrow \psi(f) \leq \psi(g)$. It is anti-extensive if $\psi(f) \leq f$ and it is extensive if $f \leq \psi(f)$. An operator is idempotent if $\psi(\psi(f)) = \psi(f)$.

The transformation ψ is applied to $f(\mathbf{x}) \in \mathcal{F}(E, \mathcal{T})$ according to the shape and size associated to the structuring element B and it is denoted as $\psi_B(f)(\mathbf{x})$.

We may now define the following ψ-complex image

$$\mathbf{f}_C(\mathbf{x}) = f(\mathbf{x}) + i\psi_B(f)(\mathbf{x}),$$

with $\mathbf{f}_C \in \mathcal{F}(E, \mathcal{T} \times i\mathcal{T})$. The data of the bivalued image are discrete complex numbers: $\mathbf{f}_C(\mathbf{x}) = \mathbf{c}_n = a_n + ib_n$, where a_n and b_n are respectively the real and the imaginary part of the complex of index n in the discrete space $\mathcal{T} \times i\mathcal{T} \subset \mathbb{C}$. Let us consider the polar representation, i.e., $\mathbf{c}_n = \rho_n \exp(i\theta_n)$, where the modulus is given by $\rho_n = |\mathbf{c}_n| = \sqrt{a_n^2 + b_n^2}$ and the phase is computed as $\theta_n = \arg(\mathbf{c}_n) = \mathrm{atan2}(b_n, a_n) = \mathrm{sign}(b_n)\,\mathrm{atan}(|b_n|/a_n)$, with $\mathrm{atan2}(\cdot) \in (-\pi, \pi]$. The phase can be mapped to $[0, 2\pi)$ by adding 2π to negative values.

Working in the polar representation, two alternative total orderings based on lexicographic cascades can be defined for complex numbers:

$$\mathbf{c}_n \leq_{\Omega_1^{\theta_0}} \mathbf{c}_m \Leftrightarrow \begin{cases} \rho_n < \rho_m \;\; or \\ \rho_n = \rho_m \;\; and \;\; \theta_n \preceq_{\theta_0} \theta_m \end{cases} ; \; \mathbf{c}_n \leq_{\Omega_2^{\theta_0}} \mathbf{c}_m \Leftrightarrow \begin{cases} \theta_n \prec_{\theta_0} \theta_m \;\; or \\ \theta_n =_{\theta_0} \theta_m \;\; and \;\; \rho_n \leq \rho_m \end{cases}$$

where $\preceq_{\theta_0}$ depends on the angular difference to a reference angle θ_0 on the unit circle, i.e.,

$$\theta_n \preceq_{\theta_0} \theta_m \;\; \Leftrightarrow \begin{cases} (\theta_n \div \theta_0) > (\theta_m \div \theta_0) \;\; or \\ (\theta_n \div \theta_0) = (\theta_m \div \theta_0) \;\; and \;\; \theta_n \leq \theta_m \end{cases}$$

such that

$$\theta_p \div \theta_q = \begin{cases} \mid \theta_p - \theta_q \mid & \text{if } \mid \theta_p - \theta_q \mid \leq \pi \\ 2\pi - \mid \theta_p - \theta_q \mid & \text{if } \mid \theta_p - \theta_q \mid > \pi \end{cases}$$

These total orderings can be easily interpreted. In $\leq_{\Omega_1^{\theta_0}}$, priority is given to the modulus, in the sense that a complex is bigger than another if its modulus is bigger, and if both have the same modulus the bigger value is the one whose phase is closer to the reference θ_0. In case of equal phase angular distances, the last condition for a total ordering is based on closeness to the phase origin, i.e., $\theta = 0$. The ordering $\leq_{\Omega_2^{\theta_0}}$ uses the same priority conditions, but they are reversed. Furthermore, by the equivalence of norms, we can state that $\rho_n \leq \rho_m \Leftrightarrow |a_n| + |b_n| \leq |a_m| + |b_m|$.

Given now a set of pixels of the initial image $[f(\mathbf{z})]_{\mathbf{z} \in Z}$, the basic idea behind our approach is to use, for instance $\leq_{\Omega_1^{\theta_0}}$, for ordering the set Z of initial pixels. Formally, we have

$$\mathbf{f}_C(\mathbf{y}) \leq_{\Omega_1^{\theta_0}} \mathbf{f}_C(\mathbf{z}) \Rightarrow f(\mathbf{y}) \preccurlyeq_{\Omega_1^{\theta_0}} f(\mathbf{z}),$$

where the *indirect total ordering* $\preccurlyeq_{\Omega_1^{\theta_0}}$ allows to compute the supremum $\widetilde{\bigvee}_{\Omega_1^{\theta_0}}$ and the infimum $\widetilde{\bigwedge}_{\Omega_1^{\theta_0}}$ in the original scalar-valued image, i.e., $\mathbf{f}_C(\mathbf{y}) = \bigvee_{\Omega_1^{\theta_0}} [\mathbf{f}_C(\mathbf{z})] \Rightarrow f(\mathbf{y}) = \widetilde{\bigvee}_{\Omega_1^{\theta_0}} [f(\mathbf{z})]$.

We notice that the complex total orderings are only defined once the transformation ψ_B is totally defined. The next question to be studied is what kind of morphological operators are useful to build basic operators such as dilations and erosions.

Adjunction and duality by complementation. The theory of adjunctions on complete lattices has played an important role in mathematical morphology [15,16,9]. The operator ε between the complete lattice $\mathcal{T}$ and itself is an erosion if $\varepsilon\left(\bigwedge_{\Omega^{\theta_0}}[f(\mathbf{x}_k)]\right) = \bigwedge_{\Omega^{\theta_0}}\varepsilon\left([f(\mathbf{x}_k)]\right)$, $k \in I$, for every function $f \in \mathcal{F}(E,\mathcal{T})$. A similar dual definition holds for dilation δ (i.e., commutation with the supremum). The pair (ε, δ) is called an adjunction between $\mathcal{T} \rightarrow \mathcal{T}$ iff $\delta\left(f\right)(\mathbf{x}) \leq_{\Omega^{\theta_0}} g(\mathbf{x}) \Leftrightarrow f(\mathbf{x}) \leq_{\Omega^{\theta_0}} \varepsilon\left(f\right)(\mathbf{x})$. If we have an adjunction for the ordering Ω^{θ_0}, the products of (ε, δ) such as the openings and the closings can be defined in a standard way. Hence, it is important that the proposed complex erosions/dilations verifies the property of adjunction.

One of the most interesting properties of standard grey-level morphological operators is the duality by the complementation $\complement$. The complement image (or negative image) $\complement f$ is defined as the reflection of f with respect to $t_{\max}/2$; i.e., $\complement f(\mathbf{x}) = t_{\max} - f(\mathbf{x}) = f^c(\mathbf{x})$, $\forall \mathbf{x} \in E$. Let the pair (ε, δ) be an adjunction, the property of duality holds that $\varepsilon(f^c) = \left(\delta(f)\right)^c \Rightarrow \varepsilon(f) = \left(\delta(f^c)\right)^c$, and this is verified for any other pair of dual operators, such as the opening/closing. In practice, this property allows us to implement exclusively the dilation, and using the complement, to be able to obtain the corresponding erosion. In our case, the transformation $f \rightarrow \complement f \Rightarrow \mathbf{f}_C \rightarrow \tilde{\mathbf{f}_C} = \complement f + i\psi_B(\complement f) = \complement f + i\complement\xi_B(f)$, where $\xi_B(f) = \complement\psi_B(\complement f)$ is the dual operator of ψ_B. Note that this is different from the complement of the ψ-complex image: $\complement\mathbf{f}_C = \complement f + i\complement\psi_B(f)$.

Ordering invariance and commutation under anamorphosis. The concepts of ordering invariance and of commutation of sup and inf operators under intensity image transformations is also important in the theory of complete lattices [11,17]. More precisely, in mathematical morphology a mapping $A : \mathcal{T} \rightarrow \mathcal{T}$ which satisfies the criterion $t \leq_\Omega s \Leftrightarrow A(t) \leq_\Omega A(s)\, \forall t, s \in \mathcal{T}$ is called an *anamorphosis*. Then, we say that the ordering $\leq_\Omega$ is invariant under A. Any increasing morphological operator ψ commutes with any anamorphosis, i.e., $\psi_B\left(A(f)\right) = A\left(\psi_B(f)\right)$. It is well known for the grey-tone case that any strictly increasing mapping A is an anamorphosis.

A typical example is the linear transformation $A(t) = K(t)$ if $0 \leq K(t) \leq t_{\max}$, $A(t) = 0$ if $K(t) < 0$ and $A(t) = t_{\max}$ if $K(t) > t_{\max}$, where $K(t) = \alpha t + \beta$, with $\alpha \geq 0$. In our case, we have for the ψ-complex image: $f \rightarrow f' = A(f) \Rightarrow \mathbf{f}_C \rightarrow \mathbf{f}'_C = A(f) + i\psi_B(A(f)) = A(f) + iA\left(\psi_B(f)\right)$, i.e., both axes of complex plane are modified according to the same mapping (scaled and shifted for the example of the linear transformation). Obviously, the partial ordering according to the modulus is invariant under A. The partial ordering with respect to the phase is also invariant if θ is defined in the first quadrant. Hence, the orderings $\Omega_1^{\theta_0}$ and $\Omega_2^{\theta_0}$ commutes with anamorphosis applied on the scalar function f.

γ-complex dilation and φ-complex erosion. A morphological filter is an increasing operator that is also idempotent (i.e., erosion and dilation are not idempotent). The two basic morphological filters, the opening γ_B and the closing φ_B, seem particularly appropriate to build the ψ-complex image. Besides the idempotence, the opening (closing) is an anti-extensive (extensive) operator which removes bright structures and peaks of intensity (dark structures and valleys of intensity) that are thinner than the structuring element B, the structures larger than B preserve their intensity values.

Let us use the diagram depicted in Fig. 1(a) for illustrating how the complex values are ordered. If we consider for instance $\psi \equiv \gamma$ and $\Omega_1^{\theta_0}$, the pixels in structures invariant according to B have module values which are bigger than pixels having the same initial grey value but belonging to structures that do not match B. In the diagram, $\mathbf{c}_1$ is bigger than $\mathbf{c}_3$, but for $\mathbf{c}_1$ and $\mathbf{c}_2$ which have the same modulus, a reference θ_0 is needed. By the anti-extensivity, we have $f(\mathbf{x}) \geq \gamma_B(f)(\mathbf{x})$ and hence $0 \leq \theta \leq \pi/4$. By taking $\theta_0 = \pi/2$, we consider that, with equal modulus, a point is bigger than another if the intensities before and after the opening are more similar (i.e., more invariant). Or in other words, when the ratio $\gamma_B(f)(\mathbf{x})/f(\mathbf{x})$ is closer to 1 or θ is closer to $\pi/4$, and consequently to $\pi/2$. This implies that the opening is an appropriate transformation to define a dilation which propagate the bright intensities associated in priority to B-invariant structures.

The same analysis leads to easily justify the choice of $\psi \equiv \varphi$ and $\Omega_1^{\pi/2}$ for the complex erosion. Note that now $\varphi_B(f)(\mathbf{x})/f(\mathbf{x}) \geq 1 \Rightarrow \pi/4 \leq \theta \leq \pi/2$. By taking the reference $\theta_0 = \pi/2$, the idea of intensities invariance before and after the closing is again used, in the ordering by θ, for considering now that a point is smaller than another if both have the same modulus and the first is closer to $\theta_0 = \pi/4$ than the second (in the example of Fig. 1(a), $\mathbf{c}_5$ is smaller than $\mathbf{c}_4$).

Mathematically, the γ-*complex dilation* is defined by

$$\begin{cases} \mathbf{f}_C(\mathbf{x}) = f(\mathbf{x}) + i\gamma_{B_C}(f)(\mathbf{x}), \\ \delta_{\langle \gamma_{B_C}, B\rangle}(f)(\mathbf{x}) = \{f(\mathbf{y}) : \mathbf{f}_C(\mathbf{y}) = \bigvee_{\Omega_1^{\pi/2}}[\mathbf{f}_C(\mathbf{z})], \mathbf{z} \in B(\mathbf{x}))\}. \end{cases}$$

and the dual φ-*complex erosion* is formulated as follows:

$$\begin{cases} \mathbf{f}_C(\mathbf{x}) = f(\mathbf{x}) + i\varphi_{B_C}(f)(\mathbf{x}), \\ \varepsilon_{\langle \varphi_{B_C}, B\rangle}(f)(\mathbf{x}) = \{f(\mathbf{y}) : \mathbf{f}_C(\mathbf{y}) = \bigwedge_{\Omega_1^{\pi/2}}[\mathbf{f}_C(\mathbf{z})], \mathbf{z} \in B(\mathbf{x}))\}. \end{cases}$$

The complex operator requires two independent structuring elements: B_C associated to the imaginary part; and B which is properly the structuring element of the complex transformation. Obviously, B_C and B can have different size and shape.

The pair $\left(\delta_{\langle \gamma_{B_C}, B\rangle}, \varepsilon_{\langle \varepsilon_{B_C}, B\rangle}\right)$ is an *adjunction*, i.e., $\delta_{\langle \gamma_{B_C}, B\rangle}(f)(\mathbf{x}) \preccurlyeq_{\Omega_1^{\pi/2}} g(\mathbf{x}) \Leftrightarrow f(\mathbf{x}) \preccurlyeq_{\Omega_1^{\pi/2}} \varepsilon_{\langle \varphi_{B_C}, B\rangle}(g)(\mathbf{x})$, for any $f, g \in \mathcal{F}(E, \mathcal{T})$. The proof is as follows. We consider the values of points $\mathbf{z} \in B(\mathbf{x})$, and we have $\bigvee_{\Omega_1^{\pi/2}}[\mathbf{f}_C(\mathbf{z})] \leq_{\Omega_1^{\pi/2}} \mathbf{g}_C(\mathbf{x}) \Leftrightarrow \bigvee_{\Omega_1^{\pi/2}}[f(\mathbf{z}) + i\gamma_{B_C}(f)(\mathbf{z})] \leq_{\Omega_1^{\pi/2}} g(\mathbf{x}) + i\gamma_{B_C}(g)(\mathbf{x}) \Leftrightarrow f(\mathbf{x}) + i\gamma_{B_C}(f)(\mathbf{x}) \leq_{\Omega_1^{\pi/2}} g(\mathbf{x}) + i\gamma_{B_C}(g)(\mathbf{x}) \leq_{\Omega_1^{\pi/2}} g(\mathbf{x}) + i\varphi_{B_C}(g)(\mathbf{x})$. On the other hand, we have $f(\mathbf{x}) + i\varphi_{B_C}(f)(\mathbf{x}) \leq_{\Omega_1^{\pi/2}} \bigwedge_{\Omega_1^{\pi/2}}[g(\mathbf{z}) + i\varphi_{B_C}(g)(\mathbf{z})] \Leftrightarrow f(\mathbf{x}) + i\gamma_{B_C}(f)(\mathbf{x}) \leq_{\Omega_1^{\pi/2}} f(\mathbf{x}) + i\varphi_{B_C}(f)(\mathbf{x}) \leq_{\Omega_1^{\pi/2}} g(\mathbf{x}) + i\varphi_{B_C}(g)(\mathbf{x})$. Consequently, we establish that $\bigvee_{\Omega_1^{\pi/2}}[\mathbf{f}_C(\mathbf{z})] \leq_{\Omega_1^{\pi/2}} \mathbf{g}_C(\mathbf{x}) \Leftrightarrow \mathbf{f}_C(\mathbf{x}) \leq_{\Omega_1^{\pi/2}} \bigwedge_{\Omega_1^{\pi/2}}[\mathbf{g}_C(\mathbf{z})]$.

In addition, if we apply the dilation to the complemented original image, we have $\bigvee_{\Omega_1^{\pi/2}}[f^c(\mathbf{z}) + i\gamma_{B_C}(f^c)(\mathbf{z})] = \bigvee_{\Omega_1^{\pi/2}}[f^c(\mathbf{z}) + i\varphi^c_{B_C}(f)(\mathbf{z})] = \left[\bigwedge_{\Omega_1^{\pi/2}}[f^c(\mathbf{z}) + i\varphi^c_{B_C}(f)(\mathbf{z})]^c\right]^c = \left[\bigwedge_{\Omega_1^{\pi/2}}[f(\mathbf{z}) + i\varphi_{B_C}(f)(\mathbf{z})]\right]^c$, $\mathbf{z} \in B(\mathbf{x})$. Hence, we have the following classical result of *duality*: $\delta_{\langle\gamma_{B_C},B\rangle}(f) = \left[\varepsilon_{\langle\varphi_{B_C},B\rangle}(f^c)\right]^c$.

It should be remarked that the dilation is extensive according to the ordering $\Omega_1^{\pi/2}$: $f(\mathbf{x}) \preccurlyeq_{\Omega_1^{\pi/2}} \delta_{\langle\gamma_{B_C},B\rangle}(f)(\mathbf{x})$, but not necessarily according to the standard ordering: $f(\mathbf{x}) \nleq \delta_{\langle\gamma_{B_C},B\rangle}(f)(\mathbf{x})$. If this last property is required for any reason, we can define the *γ-complex upper dilation* as:

$$\widehat{\delta}_{\langle\gamma_{B_C},B\rangle}(f)(\mathbf{x}) = \delta_{\langle\gamma_{B_C},B\rangle}(f)(\mathbf{x}) \vee f(\mathbf{x}).$$

Using the standard infimum $\wedge$, the dual definition leads to the *φ-complex lower erosion* $\widehat{\varepsilon}_{\langle\phi_{B_C},B\rangle}(f)(\mathbf{x})$, which is anti-extensive according to the grey level ordering.

As we show below, because they constitute an adjunction, the γ-complex dilation and the φ-complex erosion can be combined to construct derived γ,φ-complex operators such as gradients, openings/closing and even geodesic operators (e.g., opening by reconstruction, leveling, etc.). Instead of a morphological opening/closing for the γ-complex dilation and the φ-complex erosion, any other pair of anti-extensive extensive dual transformation can play a similar role, e.g. opening/closing by reconstruction, or thinning/thickening which are not idempotent operators. It is also possible to consider the ordering $\Omega_2^{\theta_0}$ for computing a complex dilation and erosion where the complex part is an opening or a closing respectively. However, we prefer to illustrate other possible ways for introducing the complex part.

τ^+-complex dilation and τ^--complex erosion. Let us consider another family of complex dilation/erosion using now the residues of the opening/closing. We remind that the top-hat and the dual top-hat are respectively the residue of the opening and the closing [12], i.e., $\tau_B^+(f)(\mathbf{x}) = f(\mathbf{x}) - \gamma_B(f)(\mathbf{x})$ and $\tau_B^-(f)(\mathbf{x}) = \varphi_B(f)(\mathbf{x}) - f(\mathbf{x})$. The top-hat transformations yield positive grey-level images and are used to extract contrasted components (i.e., smaller than the structuring element used for the opening/closing) with respect to the background and removing the slow trends. The top-hat is an idempotent transformation and if $f(\mathbf{x}) \geq 0$ then $\tau^+(f)(\mathbf{x})$ is anti-extensive and $[\tau^-(f)]^c(\mathbf{x})$ is extensive.

We introduce, with the help of the top-hats, the τ^+-complex dilation as

$$\begin{cases} \mathbf{f}_C(\mathbf{x}) = f(\mathbf{x}) + i\tau^+_{B_C}(f)(\mathbf{x}), \\ \delta_{\langle\tau^+_{B_C},B\rangle}(f)(\mathbf{x}) = \{f(\mathbf{y}) : \mathbf{f}_C(\mathbf{y}) = \bigvee_{\Omega_2^{\pi/4}}[\mathbf{f}_C(\mathbf{z})], \mathbf{z} \in B(\mathbf{x}))\}. \end{cases}$$

and the equivalent τ^--complex erosion defined by

$$\begin{cases} \mathbf{f}_C(\mathbf{x}) = f(\mathbf{x}) - i[\tau^-_{B_C}(f)]^c(\mathbf{x}), \\ \varepsilon_{\langle\tau^-_{B_C},B\rangle}(f)(\mathbf{x}) = \{f(\mathbf{y}) : \mathbf{f}_C(\mathbf{y}) = \bigwedge_{\Omega_2^{-\pi/4}}[\mathbf{f}_C(\mathbf{z})], \mathbf{z} \in B(\mathbf{x}))\}. \end{cases}$$

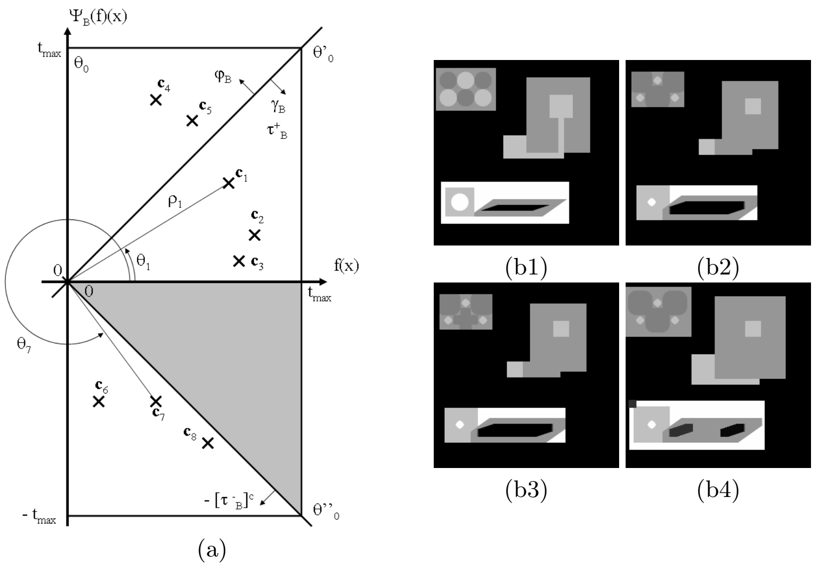

Fig. 1. (a) Complex plane for points $\in f(\mathbf{x}) + i\psi_B(f)(\mathbf{x})$. Standard erosion vs. complex erosions: (b1) original image f, (b2) erosion $\varepsilon_B(f)(\mathbf{x})$, (b3) φ-complex erosion $\varepsilon_{\langle \varphi_{B_C}, B\rangle}(f)(\mathbf{x})$, (b4) τ^--complex erosion $\varepsilon_{\langle \tau^-_{B_C}, B\rangle}(f)(\mathbf{x})$. For the three examples B is a square of size 10 pixels and B_C is a square of 40 pixels.

We must remark that for the τ^--erosion $\mathbf{f}_C \in \mathcal{F}(E, \mathcal{T} \times -i\mathcal{T})$. We can use again the diagram of Fig. 1(a) to interpret these operators. By using the ordering $\Omega_2^{\theta_0}$, the supremum favours the complex points closer to $\pi/4$ which correspond to those where the initial intensity is more similar to the intensity of the top-hat (the point $\mathbf{c}_1$ is bigger than the points $\mathbf{c}_2$ and $\mathbf{c}_3$); or in other words, the points belonging to structures well contrasted with respect to B_C. The intensity itself has only a secondary influence which is introduced by the modulus (second condition in the lexicographic ordering $\Omega_2^{\theta_0}$). In the case of the erosion, a point is smaller than another is the θ of the first is closer to $-\pi/4$ than the θ of the second. In the diagram, $\mathbf{c}_7$ is smaller than $\mathbf{c}_6$ and $\mathbf{c}_8$ is the smallest between the three (even if $\mathbf{c}_8$ presents the biggest initial intensity). In summary, by means of the τ^+-complex dilation and τ^--complex erosion, we obtain a mechanism of filtering based on the local contrast of structures and the expected results should be quite different of the standard dilation and erosion. Due to the fact that the modulus of the complex number at point x is strongly correlated to its initial intensity at x, the γ-complex dilation and φ-complex erosion lead to filtering effects more similar to the standard ones. This analysis is illustrated by the comparative example of erosion depicted in Fig. 1(b). The properties of the pair of operators $\left(\delta_{\langle \tau^+_{B_C}, B\rangle}, \varepsilon_{\langle \tau^-_{B_C}, B\rangle}\right)$ cannot be explored in detail by the limited length of the paper.

3 Generalisation to Multi-operator Cases Using Real Quaternions

We generalise the ideas introduced above by the extension to image representations based on hypercomplex numbers or real quaternions. Before that, we remind the foundations of quaternions.

Remind on quaternionic representations. A quaternion $\mathbf{q} \in \mathbb{H}$ may be represented in hypercomplex form as $\mathbf{q} = a + bi + cj + dk$, where a, b, c and d are real. A quaternion has a *real part or scalar part*, $S(\mathbf{q}) = a$, and an *imaginary part or vector part*, $V(\mathbf{q}) = bi + cj + dk$, such that the whole quaternion may be represented by the sum of its scalar and vector parts as $\mathbf{q} = S(\mathbf{q}) + V(\mathbf{q})$. A quaternion with a zero real/scalar part is called a *pure quaternion*. The addition of two quaternions, $\mathbf{q}, \mathbf{q}' \in \mathbb{H}$, is defined as follows $\mathbf{q}+\mathbf{q}' = (a+a')+(b+b')i+(c+c')j + (d + d')j$. The addition is commutative and associative. The quaternion result of the *product of two quaternions* $\mathbf{q}'' = \mathbf{q}\mathbf{q}' = S(\mathbf{q}'') + V(\mathbf{q}'')$ can be written in terms of dot product $\cdot$ and cross product $\times$ of vectors as $S(\mathbf{q}'') = S(\mathbf{q})S(\mathbf{q}') - V(\mathbf{q}) \cdot V(\mathbf{q}')$ and $V(\mathbf{q}'') = S(\mathbf{q})V(\mathbf{q}') + S(\mathbf{q}')V(\mathbf{q}) + V(\mathbf{q}) \times V(\mathbf{q}')$. The multiplication of quaternions is not commutative, i.e., $\mathbf{q}\mathbf{q}' \neq \mathbf{q}'\mathbf{q}$; but it is associative.

Any quaternion may be represented in polar form as $\mathbf{q} = \rho e^{\xi\theta}$, with $\rho = \sqrt{a^2 + b^2 + c^2 + d^2}$, $\xi = \frac{bi+cj+dk}{\sqrt{b^2+c^2+d^2}} = \overline{\xi}_i i+\overline{\xi}_j j+\overline{\xi}_k k$ and $\theta = \arctan\left(\frac{\sqrt{b^2+c^2+d^2}}{a}\right)$. Then a quaternion can be rewritten in a trigonometric version as $\mathbf{q} = \rho\,(\cos\theta + \xi\sin\theta)$. In the polar formulation, $\rho = |\mathbf{q}|$ is the modulus of $\mathbf{q}$; ξ is the pure unitary quaternion associated to $\mathbf{q}$ (by the normalisation, the pure unitary quaternion discards "intensity" information, but retains orientation information), sometimes called *eigenaxis*; and θ is the angle, sometimes called *eigenangle*, between the real part and the 3D imaginary part. It is possible to describe vector decompositions using the product of quaternions. A full quaternion $\mathbf{q}$ may be decomposed about a pure unit quaternion $\mathbf{p}^u$ [5,6]: $\mathbf{q} = \mathbf{q}_\perp + \mathbf{q}_\|$, the *parallel part* of $\mathbf{q}$ according to $\mathbf{p}^u$, also called the *projection part*, is given by $\mathbf{q}_\| = S(\mathbf{q}) + V_\|(\mathbf{q})$, and the *perpendicular part*, also named the *rejection part*, is obtained as $\mathbf{q}_\perp = V_\perp(\mathbf{q})$ where $V_\|(\mathbf{q}) = \frac{1}{2}(V(\mathbf{q}) - \mathbf{p}^u V(\mathbf{q})\mathbf{p}^u)$ and $V_\perp(\mathbf{q}) = \frac{1}{2}(V(\mathbf{q}) + \mathbf{p}^u V(\mathbf{q})\mathbf{p}^u)$.

Total orderings for quaternions. Total orderings introduced initially for colour quaternions [2] can be used also to define the derived morphological transformations. Hence, we can generalise the polar-based total orderings proposed above, now named $\leq_{\Omega_1^{q_0}}$ and $\leq_{\Omega_2^{q_0}}$, by including an additional condition in the cascade associated to the distance of the eigenaxis between the quaternions n and m and a reference quaternion, i.e., $\|\xi_n - \xi_0\| \geq \|\xi_m - \xi_0\|$. Note that here the reference θ_0 is the eigenangle from the reference quaternion q_0 (and ξ_0 is the eigenaxis of the reference). The total $\leq_{\Omega_3^{q_0}}$ is defined by considering as first condition in the lexicographical cascade the distance to reference eigenangle. But we can also introduce another total ordering based on the $\|$ / $\perp$ decomposition as follows:

$$\mathbf{q}_n \leq_{\Omega_4^{\mathbf{q}_0}} \mathbf{q}_m \;\Leftrightarrow \begin{cases} |\mathbf{q}_{\parallel\, n}| < |\mathbf{q}_{\parallel\, m}| \;\; or \\ |\mathbf{q}_{\parallel\, n}| = |\mathbf{q}_{\parallel\, m}| \;\; and \;\; |\mathbf{q}_{\perp\, n}| \geq |\mathbf{q}_{\perp\, m}| \end{cases}$$

The pure unitary quaternion required for the $\parallel$ / $\perp$ decomposition is just the corresponding to the reference quaternion $\mathbf{q}_0$. The last one is only a pre-ordering, i.e., two distinct quaternions can verify the equality of the ordering. In order to have total ordering, the lexicographic cascade can be completed with a priory in the choice of the various hypercomplex components.

$\left(\boldsymbol{\Psi}^+, \boldsymbol{\Omega}_+^{\mathbf{q}_0}\right)$-hypercomplex dilation and $\left(\boldsymbol{\Psi}^-, \boldsymbol{\Omega}_-^{\mathbf{q}_0}\right)$-hypercomplex erosion. Given the four-variate transformation $\boldsymbol{\Psi} = \left(\psi_{B_0}^0, \psi_{B_I}^I, \psi_{B_J}^J, \psi_{B_K}^K\right)$, the $\boldsymbol{\Psi}$-hypercomplex image is defined as

$$\mathbf{f}_H(\mathbf{x}) = \psi_{B_0}^0(f)(\mathbf{x}) + i\psi_{B_I}^I(f)(\mathbf{x}) + j\psi_{B_J}^J(f)(\mathbf{x}) + k\psi_{B_K}^K(f)(\mathbf{x}).$$

After choosing a particular $\boldsymbol{\Psi}^+$-hypercomplex representation as well as a particular quaternionic total ordering $\Omega_+^{\mathbf{q}_0}$, one defines the $\left(\boldsymbol{\Psi}^+, \Omega_+^{\mathbf{q}_0}\right)$-hypercomplex dilation as $\delta_{\langle \Psi^+, B\rangle}(f)(\mathbf{x}) = \{f(\mathbf{y}) : \mathbf{f}_H(\mathbf{y}) = \bigvee_{\Omega_+^{\mathbf{q}_0}}[\mathbf{f}_H(\mathbf{z})], \mathbf{z} \in B(\mathbf{x})\}$. Similarly, associated to the pair $\left(\boldsymbol{\Psi}^-, \Omega_-^{\mathbf{q}_0}\right)$, a $\boldsymbol{\Psi}^-$-hypercomplex erosion is defined. We should notice that this framework generalise the complex operators introduced in previous section; e.g., $\boldsymbol{\Psi}^+ = (\mathrm{Id}, \gamma_{B_C}, 0, 0)$ and $\Omega_+^{\mathbf{q}_0} \equiv \Omega_1^{\mathbf{q}_0}$ with $\mathbf{q}_0 = 1 + i$ corresponds to the γ-complex dilation. Therefore, two kinds of degrees of freedom must be set up (i.e., the hypercomplex transformation and the quaternionic ordering, which includes the choice of the reference quaternion) to have totally stated the operator. As we show below in the examples, the four-variate transformation can be used for instance to introduce directional openings, directional top-hats or directional gradients for the imaginary part, and real counterpart being an isotropic operator which cannot be necessary the identity. This framework can be specifically exploited by working with $\Omega_4^{\mathbf{q}_0}$ and selecting the appropriate reference quaternion for the $\parallel$ / $\perp$ decomposition. The properties of these generic four-variate hypercomplex operators should be studied in depth in ongoing research.

4 Examples of Derived Morphological Operators and Applications

The hypercomplex dilations/erosions introduced in the paper can be used to build more advanced operators such as gradients, openings/closings (and their residues), alternate sequential filters; and geodesic operators, such as the openings/closings by reconstruction or the levelings. The principle entails using always a homogeneous pair of basic operators and then applying the standard definitions for the evolved operators.

In Fig. 2 are given three comparative examples of morphological filters applied to natural images. The idea is to compare the standard result with various hypercomplex operators. In the first case we calculate a symmetric gradient (i.e., dilation minus erosion) of a very noisy image. It is observed that each

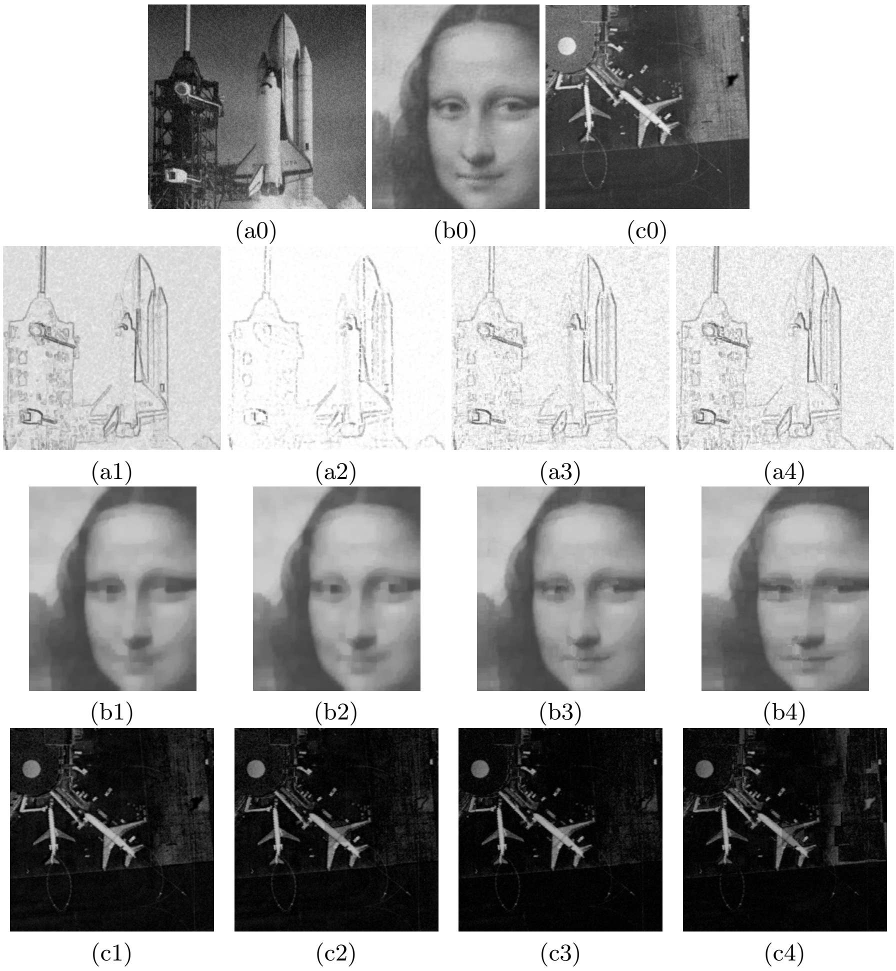

Fig. 2. First row: original images. Second row, comparison of gradient $\varrho_B(f) = \delta_B(f) - \varepsilon_B(f)$ (B is a square of 3 pixels): (a1) standard transformation, (a2) τ^+-complex dilation and τ^--complex erosion where $B_C = D_5$ is a square of size 5, (a3) $\boldsymbol{\Psi}^{+/-} = (\gamma_{B_0}/\varphi_{B_0}, \gamma_{B_I}/\varphi_{B_I}, \gamma_{B_J}/\varphi_{B_J}, 0)$, $\Omega_3^{\mathbf{q}_0}$ with $\mathbf{q}_0 = i + j$, where $B_0 = D_5$, $B_I = L_5^x$ is an horizontal line of length 5 and $B_J = L_5^y$ is an vertical line of length 5, (a4) $\boldsymbol{\Psi}^{+/-} = \left(\tau^+_{D_5}/-[\tau^-_{D_5}]^c, \tau^+_{L_5^x}/-[\tau^-_{L_5^x}]^c, \tau^+_{L_5^y}/-[\tau^-_{L_5^y}]^c, 0\right)$, $\Omega_3^{\mathbf{q}_0}$ with $\mathbf{q}_0 = i + j$. Third row, comparison of $\gamma_B\varphi_B(f)$ (B is a square of 3 pixels): (b1) standard transformation, (b2) based on γ-complex dilation and φ-complex erosion with $B_C = D_{10}$, (b3) $\boldsymbol{\Psi}^{+/-} = \left(\gamma_{D_{10}}/\varphi_{D_{10}}, \gamma_{L_{10}^x}/\varphi_{L_{10}^x}, \gamma_{L_{10}^y}/\varphi_{L_{10}^y}, 0\right)$, $\Omega_3^{\mathbf{q}_0}$ with $\mathbf{q}_0 = i + j$, (b4) idem. with $\mathbf{q}_0 = i$. Four row, comparison of top-hat τ_B^+ (B is a square of 25 pixels): (c1) standard transformation, (c2) based on γ-complex dilation and φ-complex erosion with $B_C = D_{10}$, (c3) $\boldsymbol{\Psi}^{+/-} = \left(\gamma_{D_{10}}/\varphi_{D_{10}}, \gamma_{L_{10}^x}/\varphi_{L_{10}^x}, \gamma_{L_{10}^y}/\varphi_{L_{10}^y}, 0\right)$, $\Omega_3^{\mathbf{q}_0}$ with $\mathbf{q}_0 = i + j$, (c4) $\boldsymbol{\Psi}^{+/-} = \left(\gamma_{D_{10}}/\varphi_{D_{10}}, \varrho_{L_{10}^x}/-\varrho_{L_{10}^x}, \varrho_{L_{10}^y}/-\varrho_{L_{10}^y}, 0\right)$, $\Omega_3^{\mathbf{q}_0}$ with $\mathbf{q}_0 = i + j$.

hypercomplex gradient presents particular characteristics but in any case the results are regularised with respect to the standard gradient. The second example illustrates how an alternate open/close filter is used to simplify a noisy image. We notice again that the behaviour of hypercomplex operators is quite different of standard ones, and in particular, we observe the way to introduce directional effects on the filters by decomposing the quaternions according to a particular privileged direction. The effects of a top-hat are finally compared in the last example. The aim is to remove as well as possible the background, in order to enhance the aeroplanes. As we observe, the results are better for some of the hypercomplex operators.

5 Conclusions and Perspectives

We have introduced morphological operators for grey-level images based on indirect total orderings. The orderings are associated to hypercomplex image representations where the components of the hypercomplex function are obtained from a prior transformation of the original image. The motivation was to introduce in the basic erosion/dilation operators some information on size invariance or on relative contrast of structures. The results obtained from the initial tests showed their potential applicative interest. However, a more detailed characterisation of their properties and some specific applications of these operators are currently under study. Other representations using upper dimensional Clifford Algebras [1] can be foreseen in order to have a more generic framework not limited to four-variables image representations. In addition, the approach can also be extended to already natural multivariate images (i.e., multispectral images) and, in this last case, it seems appropriate to envisage tensor representations and associated total orderings.

References

1. Ablamowicz, R., Sobczyk, G.: Lectures on Clifford (Geometric) Algebras and Applications. Birkhäuser, Basel (2004)
2. Angulo, J.: Quaternion colour representations and derived total orderings for morphological operators. In: Proc. of the CGIV 2008, pp. 417–422 (2008)
3. Bülow, T., Sommer, G.: Hypercomplex Signals - A Novel Extension of the Analytic Signal to the Multidimensional Case. IEEE Trans. Signal Proc. 49(11), 2844–2852 (2001)
4. Deng, T.Q., Heijmans, H.J.A.M.: Gray-scale Morphology Based on Fuzzy Logic. J. Math. Imaging Vision 16(2), 155–171 (2002)
5. Ell, T.A., Sangwine, S.J.: Hypercomplex Wiener-Khintchine theorem with application to color image correlation. In: IEEE ICIP 2000, vol. II, pp. 792–795 (2000)
6. Ell, T.A., Sangwine, S.J.: Hypercomplex Fourier transform of color images. IEEE Trans. Image Proc. 16(1), 22–35 (2007)
7. Felsberg, M., Sommer, G.: The Monogenic Signal. IEEE Trans. Signal Proc. 49(12), 3136–3144 (2001)

8. Felsberg, M., Sommer, G.: The monogenic scale-space: A unifying approach to phase-based image processing in scale-space. J. Math. Imaging Vision 21, 5–26 (2004)
9. Heijmans, H.J.A.M.: Morphological Image Operators. Academic Press, Boston (1994)
10. Heijmans, H.J.A.M., Keshet, R.: Inf-Semilattice Approach to Self-Dual Morphology. J. Math. Imaging Vision 17(1), 55–80 (2002)
11. Matheron, G.: Les treillis compacts. Technical Report - Paris School of Mines, N-23/90/G (1990)
12. Meyer, F.: Constrast features extraction. In: Chermant (ed.) Quantitative Analysis of Microstructures in Materials Science, Biology and Medecine, pp. 374–380. Riederer Verlag (1977)
13. Meyer, F., Angulo, J.: Micro-viscous morphological operators. In: Mathematical Morphology and its applications to Signal and Image Processing (ISMM 2007), pp. 165–176 (2007)
14. Sangwine, S.J., Ell, T.A.: Mathematical approaches to linear vector filtering of colour images. In: Proc. CGIV 2002, pp. 348–351 (2002)
15. Serra, J.: Image Analysis and Mathematical Morphology, vol. I. Academic Press, London (1982)
16. Serra, J.: Image Analysis and Mathematical Morphology. Theoretical Advances, vol. II. Academic Press, London (1988)
17. Serra, J.: Anamorphoses and Function Lattices (Multivalued Morphology). In: Dougherty (ed.) Mathematical Morphology in Image Processing, pp. 483–523. Marcel-Dekker, New York (1992)
18. Shi, L., Funt, B.: Quaternion color texture segmentation. Computer Vision and Image Understanding 107(1-2), 88–96 (2007)
19. Zang, D., Sommer, G.: Signal modeling for two-dimensional image structures. J. Vis. Commun. Image R. 18, 81–99 (2007)